Applied Physics Research; Vol. 17, No. 1; 2025
ISSN 1916-9639 E-ISSN 1916-9647
Published by Canadian Center of Science and Education

Separating Absorption and Scattering Coefficients for the Characterization of Optical Turbid Media Using Structured Laser Illumination Planar Imaging and Conventional Spectroscopy Technique

Guy-Oscar Regnima[1,2], Serge Martial Adepo[2,3], Evariste Kouamé Amany[2], Abaka Kouacou[2] & Jérémie Zoueu[2]

[1] Unité de Formation et de Recherche en Sciences et Technologie, Département de Physique, Université de Man, BP 20 Man, Côte d'Ivoire

[2] Laboratoire d'Instrumentation Image et Spectroscopie, Institut National Polytechnique Felix Houphouet-Boigny, BP 1093 Yamoussoukro, Cote d'Ivoire

[3] Laboratiore de Physique Fondamentale Appliquée (LPFA), Université Nangui Abrogoua, Unité de Formation et de Recherche des Sciences Fondamentales Appliquées, 02 BP 808 Abidjan 02, Côte d'Ivoire

Correspondence: Guy-Oscar Regnima, Unité de Formation et de Recherche en Sciences et Technologie, Département de Physique, Université de Man, BP 20 Man, Côte d'Ivoire. Tel: 225-70-735-2616. E-mail: regnimaguyoscar@gmail.com

Received: December 14, 2024 Accepted: January 17, 2025 Online Published: March 5, 2025

doi:10.5539/apr.v17n1p10 URL: https://doi.org/10.5539/apr.v17n1p10

Abstract

We report on the potential of combining the Structured Laser Illumination Planar Imaging (SLIPI) technique and optical spectroscopy for characterizing scattering and absorbing liquids. Water solutions of milk and coffee were investigated at 10 different turbidity levels. The SLIPI technique eliminates the light intensity contributions from multiply scattered photons in these solutions, enabling accurate and reliable measurements of their extinction coefficients μ_e. Optical spectroscopy, on the other hand, provides complementary insights into the interaction between light and matter, allowing precise spectral analysis. The linearity of the extinction coefficient measurements obtained using the SLIPI technique as a function of concentration, combined with spectroscopic approximations, enables the separation of absorption and scattering coefficients. This opens the possibility for precise characterization of both absorption and scattering properties in dense liquid media.

Keywords: scattering coefficient, absorption coefficient, turbid media, milk, structured illumination, spectroscopy

1. Introduction

Understanding the phenomenon of propagation and light distribution in the matter are paramount. Considering the biological tissues, the extraction of optical parameters allows us to make a medical diagnosis effective and safe in tissue therapy, planning or monitoring these tissues (Durduran, Choe, Baker, & Yodh, 2010; Patterson, Wilson, & Wyman, 1991; Patterson, Wilson, & Wyman, 1991; Star, 1997). For example, in vivo determination of the optical properties of cancerous tissues is necessary to optimize the distribution of the light dose during photodynamic therapy (Davidson et al., 2009; Moore et al., 2011; Pantelides, Whitehurst, Moore, King, & Blacklock, 1990).

As a result, the propagation of light in biological tissues, which are optically dense, where scattering and absorption phenomenons exist, can be described by the Boltzmann transport equation (Ishimaru, 1978). This involves the knowledge of four optical properties, namely: the absorption coefficient μ_a, the scattering coefficient μ_s, the reduced scattering coefficient μ_s' and phase function g.

Futhermore, there are different and non-invasive techniques that allow the determination of optical properties. In general, all these techniques used can be classified according to the type of light sources used to probe the tissues.

These light sources are divided into three categories: continuous wave sources (cw), "time resolved" sources and intensity modulation sources (Wilson, Patterson, & Burns, 1986; Patterson, Chance, & Wilson, 1989; Patterson, Wilson, & Wyman, 1991; Patterson, et al., 1991; Prahl, & Vitkin, 1992; Yoon, Ghosh, & Straight, 1993; Kienle et al., 1996; Delpy & Cope, 1997; Nichols, Hull, & Foster, 1997; Dognitz, & Wagnieres, 1998).

Regarding techniques using continuous wave sources or continuous intensity sources, these are usually associated to the determination of fluence rate measurements. From the relative measurements of fluence rate at several separation distances between the source and the detector, make possible the determination of the extinction coefficient μ_e from the value of the slope of the curve obtained (Gwamuri, Gholap, Shartir, & Bauh-Bassuah, 2014; Johansson, Axelsson, Andersson-Engels, & Swartling, 2007; Zaccanti, Bianco, & Martelli, 2003). A variation of the multi-range fluence measurements, called the Absorbent addition technique permits to obtain both the absorption and scattering coefficients by modifying the absorption coefficient by known small amounts (Wilson, Patterson, & Burns, 1986; Staveren, Moes, Marie, Prahl, & Gemert, 1991). Moreover, to obtain the absolute fluence rate measurements, complex devices calibrations are necessary. Such calibrations can be difficult to implement in vivo measurements.

The techniques that use the intensity modulation of light to measure optical properties of tissues are also well known. Cuccia et al. have developed and used for the first time an imaging technique with wide field called "spatial frequency domain imaging" or "modulated imaging" which is based on the structured illumination technique (Cuccia, Bevilacqua, Durkin, Ayers, & Tromberg, 2009). This imaging approach isolates the diffuse reflectance dependent on the frequency modulation of the sample at the level of each pixel of the image, which facilitates the analysis of the sample in the spatial frequency domain and corresponding to the extraction of optical properties (Cuccia, Bevilacqua, Durkin, & Tromberg, 2005; Cuccia, Bevilacqua, Durkin, Ayers, & Tromberg, 2009). This technique has been widely used in recent years in the field of Biomedical. Some authors have also used this technique in the agricultural field for the detection of bruises (contusion, hematoma) on apples and to measure the reduced absorption and scattering coefficients of apple fruits (Anderson, Cuccia, & Durkin, 2007; Hu, Fu, He, & Ying, 2016; Lu, Li, & Lu, 2016). The method is similar to the one we used in our study.

In this work, a technique called Structured Laser Illumination Planar Imaging (SLIPI) has been combined with the conventional spectroscopy method to characterize scattering and absorbing media by determining their absorption and scattering coefficients. Among the authors, some studies have been conducted using SLIPI technique for the characterization of atomizing sprays, to probe uniform solid–liquid dispersions (Kristensson et al., 2011) and to measure temperature in liquids (Mishra, Abou, Polster, Kristensson, & Berrocal, 2016). Recently, the single-phase SLIPI approach combined with chemometric analysis is employed to measure the extinction coefficient in different coffee solutions (Bagui, Kaduki, Berrocal & Zoueu, 2016; Koffi et al. 2017). It has also been used as a tool for diagnosis of the state of the power transformers oils for their deterioration and aging (Regnima et al. 2017). A comparative study between the technique of optical absorption spectroscopy and the single-phase SLIPI approach has been made by Regnima et al. (2017). Through this experiment, it is noted that SLIPI technique has demonstrated its ability to measure the exact value of the extinction coefficient in dense solutions, where the commercial absorption spectrometers fail. Reliable measurements of SLIPI applied to the solutions have been obtained for values of extinction coefficients. The linearity of the extinction coefficient measurements obtained from SLIPI technique according to concentration was used for the separation of the absorption and scattering coefficients. From this following study, we believe that the results will be helpful for researcher's future investigations, and for scientifics community, to improve the efficiency of their research.

2. Material and Methods

2.1 Preparation of the Probed Solutions

The milk solutions are prepared using evaporated milk (from the brand "Bonnet Rouge") characterized by more than 9% fat content. A solution S_1 with concentration C_1 is created by diluting 5 ml of milk within 495 ml of water. This dilution results in a concentration equal to 1% from the initial milk concentration C_0. Based on this first dilution of concentration C_1, ten others solutions have been prepared to obtain a linear decrease in milk concentration from solution S_3 to preserve SLIPI linearity. A detailed description of this dilution procedure is given in Table 1. The resulting 10 solutions are shown in Figure 1.

For milk solutions, its white color indicates that scattering is highly dominant in comparison to absorption through the entire visible wavelength range. Milk is a very complex food consisting of an emulsion of fat globules in suspension in a water solute. The size of the fat globules is larger than the wavelength and ranges

around 2 μm in diameter (Ménard et al., 2010). As a result, when light interact with such particles, the angular distribution of the scattered radiation is governed by the Lorenz–Mie theory. In such cases, light does not scatter equally in all directions but mostly in the forward direction. This differs from the coffee solutions, where light is interacting with molecules of size much smaller than that of the incident wavelength, resulting in a Rayleigh scattering process.

Table 1. Protocol for the preparation of different milk solution samples

		Milk solutions
Solutions	Milk dilutions	Concentrations (g/l)
S_1	V_1=5 ml milk + 495 ml water	C_1
S_2	V_2=67.5 ml of V_1 + 7.5 ml water	$C_2 = 0.9C_1$
S_3	V_2=60.0 ml of V_1 + 15.0 ml water	$C_3 = 0.8C_1$
S_4	V_2=52.5 ml of V_1 + 22.5 ml water	$C_4 = 0.7C_1$
S_5	V_2=45 ml of V_1 + 30.0 ml water	$C_5 = 0.6C_1$
S_6	V_2=37.5 ml of V_1 + 37.5 ml water	$C_6 = 0.5C_1$
S_7	V_2=30.0 ml of V_1 + 45.0 ml water	$C_7 = 0.4C_1$
S_8	V_2=22.5 ml of V_1 + 52.5 ml water	$C_8 = 0.3C_1$
S_9	V_2=15.0 ml of V_1 + 60.0 ml water	$C_9 = 0.2C_1$
S_{10}	V_2=7.5 ml of V_1 + 67.5 ml water	$C_{10} = 0.1C_1$

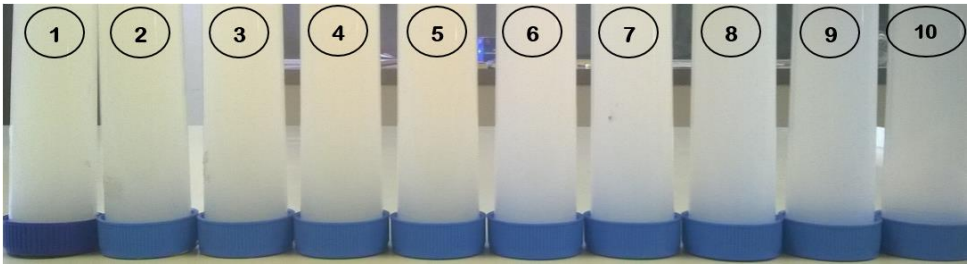

Figure 1. Photographs of the samples prepared at various dilution ratios for the milk. The increase in turbidity from right to left is apparent

The coffee solutions are prepared using instant coffee made of 100% robusta coffee. An initial solution C_1 has been by dissolving 6 g of coffee into 450 ml of water. From this solution, nine solutions have been, once again, prepared to obtain a linear decrease in concentration, in a similar fashion that for the milk solutions. A detailed description of this dilution procedure is given in Table 2.

The resulting 10 solutions are shown in Figure 2. At high concentrations, the coffee solution appears black due to the important absorption from the coffee molecules. This is particularly true for the blue and green spectral regions. However, at low concentrations, the coffee solutions appear "yellowish–reddish," indicating that scattering is not negligible and also occurs in this spectral range.

Table 2. Protocol for the preparation of different coffee solution samples

		Coffee solutions
Solutions	Coffee dilutions	Concentrations (g/l)
S_1	V_1=6 g coffee + 450 ml water	$C_1 = m_1/V_1$
S_2	V_2=67.5 ml of V_1 + 7.5 ml water	$C_2 = 0.9C_1$
S_3	V_2=60.0 ml of V_1 + 15.0 ml water	$C_3 = 0.8C_1$

S_4	V_2=52.5 ml of V_1 + 22.5 ml water	$C_4 = 0.7C_1$
S_5	V_2=45 ml of V_1 + 30.0 ml water	$C_5 = 0.6C_1$
S_6	V_2=37.5 ml of V_1 + 37.5 ml water	$C_6 = 0.5C_1$
S_7	V_2=30.0 ml of V_1 + 45.0 ml water	$C_7 = 0.4C_1$
S_8	V_2=22.5 ml of V_1 + 52.5 ml water	$C_8 = 0.3C_1$
S_9	V_2=15.0 ml of V_1 + 60.0 ml water	$C_9 = 0.2C_1$
S_{10}	V_2=7.5 ml of V_1 + 67.5 ml water	$C_{10} = 0.1C_1$

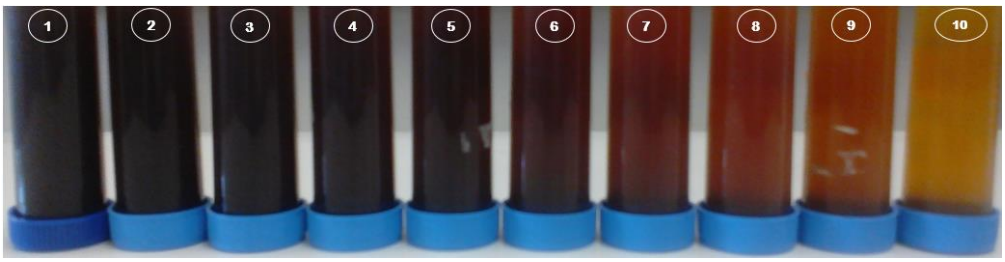

Figure 2. Photographs of the samples prepared at various dilution ratios for the coffee. The increase in turbidity from right to left is apparent

2.2 Overview on the Conventional Absorption Spectroscopy Technique

An optical spectrometry device from Ocean Optics was used to acquire the absorbance spectra of samples. A detailed description of this device is given in our previous work (Regnima et al., 2017). Figure 3 shows a detailed diagram where white LED light source is used to probe the solutions placed in a cuvette. The transmitted light is then spectrally dispersed and analyzed using the USB4000-FL spectrometer. A computer connected to the spectrophotometer is used to display the absorption spectra of each probed sample.

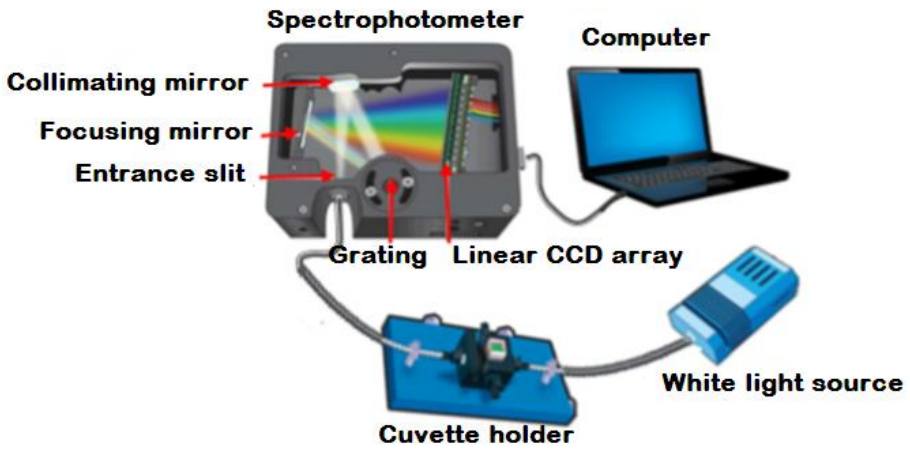

Figure 3. Illustration adapted from Ocean Optics of the absorption spectrophotometer. White light source exits the first optical fiber at the focus of a collimating lens. The collimated white beam crosses the turbid solution and is collected using another lens, focusing it into a second optical fiber. This light is then spectrally dispersed and analyzed using the USB4000-FL spectrometer from Ocean Optics.

First, the transmitted light I_0 is recorded using a "blank" reference cuvette containing only the solvent. Then, the transmitted light I_t t is recorded, where both the solvent and the solute are mixed. Thus, the absorption of

the solute only can be quantified by taking the ratio between the two measurements. This corresponds to the transmittance T, which is a measure of the light attenuation along the distance L of the cuvette. According to the Beer–Lambert–Bouguer law and assuming a collimated beam of a single wavelength crossing a uniform medium, the transmittance T is given by

$$T = {I_t}/{I_0} = e^{-\mu_e L} \tag{1}$$

where μ_e(mm^{-1}) is the extinction coefficient and L(mm) is the width of the cuvette containing the probed solution.

Using equation 1, the extinction coefficient μ_e is extracted as

$$\mu_e = -\ln(T)/L \tag{2}$$

2.3 Single Phase SLIPI Approach

2.3.1 Measurements Principle

The single-phase SLIPI approach used in the current study is based on an analytical tool known as lock-in detection (Meade, 1982). Lock-in detection is most often associated with analysis of temporally varying signals, but it works equally well for spatially modulated signals. To explain the principle of lock-in detection, consider a 1D signal, *I(x)*, with a superimposed periodic variation of amplitude I_S in space:

$$I(x) = I_S \sin(2\pi\vartheta x + \varphi) + I_{MS}(x) \tag{3}$$

where ϑ equals the spatial frequency (mm^{-1}) of the modulation and φ is the spatial phase, which is unknown. The I_{MS} term represents any unwanted non-modulated intensity contribution also being detected, such as multiple light scattering or any surrounding light background. The purpose of the lock-in analysis is to extract I_S and reject I_{MS}. To achieve this end, the signal $I(x)$ is multiplied with two reference signals R_1 and R_2, created computationally, that have a relative phase shift of ${\pi}/{2}$:

$$R_1(x) = \sin(2\pi\vartheta x) \text{ and } R_1(x) = \sin(2\pi\vartheta x) \tag{4}$$

Multiplying $I(x)$ with these reference signals yields

$$I_1(x) = {1}/{2}\, I_S(\cos(\varphi) - \cos(4\pi\vartheta x + \varphi)) + I_{MS}\sin(2\pi\vartheta x)) \tag{5}$$

$$I_2(x) = {1}/{2}\, I_S(\sin(\varphi) + \sin(4\pi\vartheta x + \varphi)) + I_{MS}\cos(2\pi\vartheta x)) \tag{6}$$

The frequency analysis of I_1 and I_2 reveals three components: (1) a DC component, (2) one modulated with 2ϑ, and (3) one modulated with ϑ. The two latter components can be suppressed by means of a low-pass filter in the Fourier domain, with a cutoff frequency less than ϑ, resulting in the following expressions:

$$\tilde{I}_1(x) = {1}/{2}\, \tilde{I}_S\cos(\varphi) \text{ and } \tilde{I}_2(x) = {1}/{2}\, \tilde{I}_S\sin(\varphi) \tag{7}$$

where the tilde assignment indicates the applied frequency filtering. From these, $\tilde{I}_S$ can finally be extracted by calculating

$$\tilde{I}_S = 2\sqrt{(\tilde{I}_1)^2 + (\tilde{I}_2)^2} \tag{8}$$

An illustration of the single-phase SLIPI process is given in Figure 4.

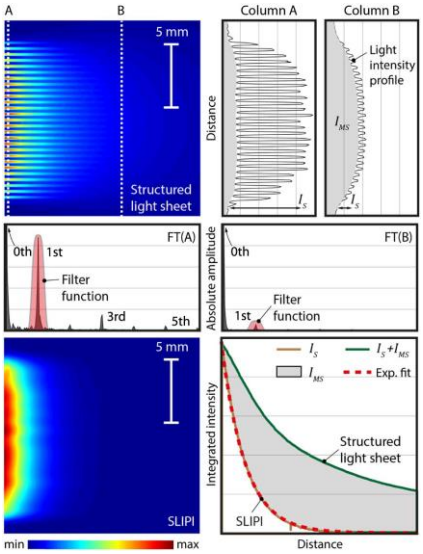

Figure 4. Principle of single-phase SLIPI. The example shows the signal from a structured laser sheet with cross sections extracted from two different depths, marked as A and B. Notice the decrease in amplitude from column A to B. The 1D Fourier transforms of curves A and B show the reduction in strength of the first-order peak (modulation frequency). This frequency is then isolated using frequency filtering (red area) after applying the lock-in algorithm. Finally, the exponential decay is revealed, as shown in the SLIPI image and related curve IS.

From a modulated image, the amplitude of the modulation is extracted using Equation (8). The modulated component I_S corresponds to the single light scattering, which reduces exponentially with distance. By applying an exponential fit to I_S, the extinction coefficient, μ_e, can be directly extracted as stated in the Beer–Lambert–Bouguer law using equation (1).

2.3.2 Optical Set up and Measurements

The light sources consist of two continuous-wave (CW) laser beams of 450 nm and 638 nm, which are recombined along the same optical path using a dichroic mirror. One laser is activated at a time and a neutral density wheel is used to adjust the incident irradiance in order to optimize the signal-to-noise ratio while avoiding saturation. The beam is then expanded by a factor of $\times 10$ using a telescope arrangement made of a pair of positive spherical lenses. An aperture is used to select the central part of the beam where the spatial intensity profile is fairly homogeneous. A positive cylindrical lens of a 200 mm focal lens is used to create the light sheet into the cuvette. To spatially modulate this light sheet, a Ronchi grating of 5 lp $/$ mm is directly fixed onto a cuvette of 20 mm width. Thus, perfect modulation is created just at the entrance of the cuvette, limiting unwanted effects caused by near-field diffractions known as the Talbot effect (Talbot, 1836).

In order to reduce signal attenuation as light propagates from the structured light sheet toward the camera, the location of the illumination plane is fixed as close as possible from the cuvette glass wall ($\sim$2 mm) facing the camera. The images are recorded using a 14 bit electron-multiplying- (EM) CCD camera, Luca (r) from Andor, and the final image is the result of the accumulation over 200 single-shot images. The exposure time of the camera objective ranges between 0.001 and 0.01 s to optimize the dynamic range for each concentration cases. The more diluted solutions were generating a lower signal than the more concentrated ones, having, therefore, longer exposure times. A detailed schematic of the optical setup is given in Figure 5.

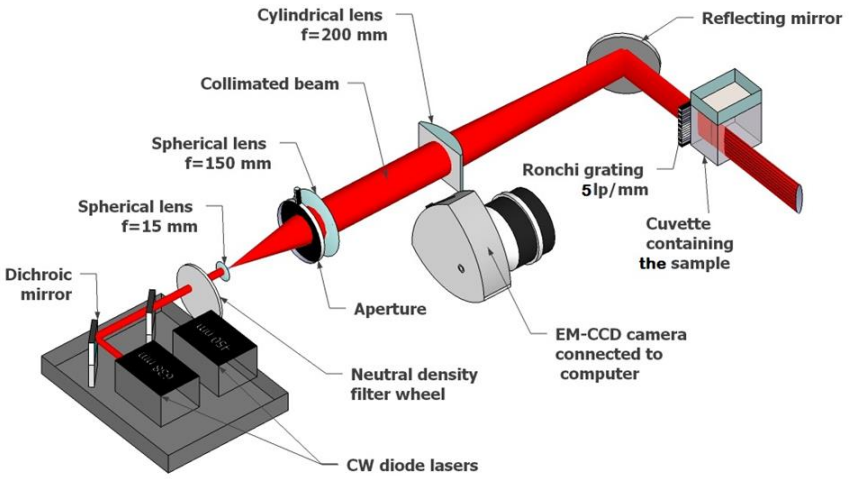

Figure 5. SLIPI optical setup. After expanding the incident laser beam, a light sheet is formed by using a cylindrical lens focusing the beam into the cuvette. The light sheet is modulated just prior to entering the cuvette containing the turbid liquid by a Ronchi grating of 5 lp ⁄ mm frequency. The images are recorded using an EM-CCD camera.

2.4 Implementation of the Spectrometer-SLIPI Combination Technique

Spectroscopic measurements show linearity between extinction coefficient and concentration for dilute solutions as previously demonstrated (Regnima et al., 2017). This simply reflects a proportionality between the absorption or scattering coefficient and the concentration for dilute solutions.

Indeed, the approximation is made that in the probed medium the single scattering regime is assumed. In this case, the optical depth (OD) is less than one (OD $\leqslant$ 1). Thus, in the linear part, if the probed medium is predominantly absorbing, we have the following relationship (Moes, van-Gemert, Star, Marijnissen, & Prahl, 1989; Michels, Foschum, & Kienle, 2008):

$$\mu_e \approx \mu_a = \alpha * C \tag{9}$$

where μ_e, μ_a, α and C are respectively the extinction coefficient, the absorption coefficient, the slope of the linearity line and the concentration of the solution S_i considered.

On the other hand, if the medium is predominantly scattering, then relation (9) becomes (Moes, van-Gemert, Star, Marijnissen, & Prahl, 1989; Michels, Foschum, & Kienle, 2008):

$$\mu_e \approx \mu_s = \alpha * C \tag{10}$$

where μ_s is the scattering coefficient.

Thus, for dilute solutions, the measured values of the extinction coefficient in the linear part correspond to the values of the absorption or scattering coefficients depending on the nature of these solutions. By combining the SLIPI technique and the spectroscopic technique, the difference between the extinction coefficients measured with the SLIPI and the spectrometer in the linear part is very small because of the similarity of the results.

For high turbidity solutions where linearity is lost, the determination of the absorption or scattering coefficient is described as follows:

First, a linear extrapolation is made from the equation of the line where the linearity of the spectroscopic measurements is observed. This will allow the determination of the absorption or scattering coefficients depending on the nature of solution. After determining one of the coefficients, the other coefficient is determined as follows:

- The solution S_i from which the spectroscopic measurements lose their linearity is chosen.

- The difference of the extinction coefficient obtained in SLIPI and in the spectrometer is measured for this solution S_i. This difference is either the scattering coefficient of the solution S_i in the case of a strongly absorbing solution, or the absorption coefficient for a strongly scattering solution.

- Moreover, there is a proportionality between the different extinction coefficients. Similarly, this proportionality is also verified for the absorption and scattering coefficients (Narasimhan et al., 2006). Thus, from the determination of the scattering or absorption coefficient of the solution S_i, one can trace back to the determination of the absorption or scattering coefficients of the other solutions of high turbidity.

In our previous works, a Ronchi grating of 2 lines per millimeter (2 lp / mm) was used to spatially modulate the laser light sheet. In the present study, a Ronchi grating of 5 lp / mm directly attached to the tank has been used because preview studies have demonstrated that there is a very throng similarity in results between single phase SLIPI technique and spectrometry technique by using a Ronchi grating of 5 lp / mm (Koffi et al., 2019).

A telecentric lens were chosen. The use of the telecetric lens makes it possible to obtain the smallest details at the pixel level during image acquisition. It also has the advantage of effectively removing the geometric aberrations.

3. Results

3.1 Coffee Results

The results obtained are presented in the following section. The spectra acquired with the USB 4000-FL spectrometer are given in Figure 6 (a).

The resulting images of the SLIPI-1p measurements are given in Figure 6 (b). The dilution cases of solutions 1 to 5 have been chosen here, for illustration, at an illumination wavelength of 638 nm. The column of images on the left-hand side corresponds to the recorded raw images. In graphs 1 (a) and 1 (b), the evolution of the extinction coefficient as a function of the concentration has been plotted for the spectroscopic and SLIPI measurements respectively.

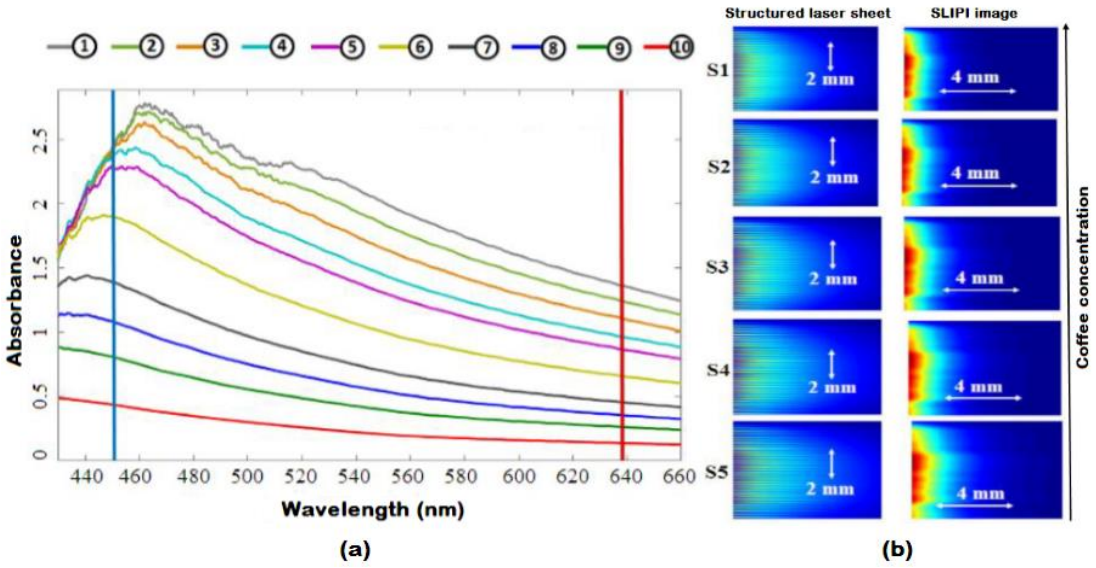

Figure 6. Absorbance spectra of the coffee solutions measured using absorption spectrophotometry in (a). The increase of the absorbance with concentration is clearly seen. In (b), images of the structured light sheet crossing the cuvette at increased coffee concentration. The corresponding SLIPI images are given on the right-hand side.

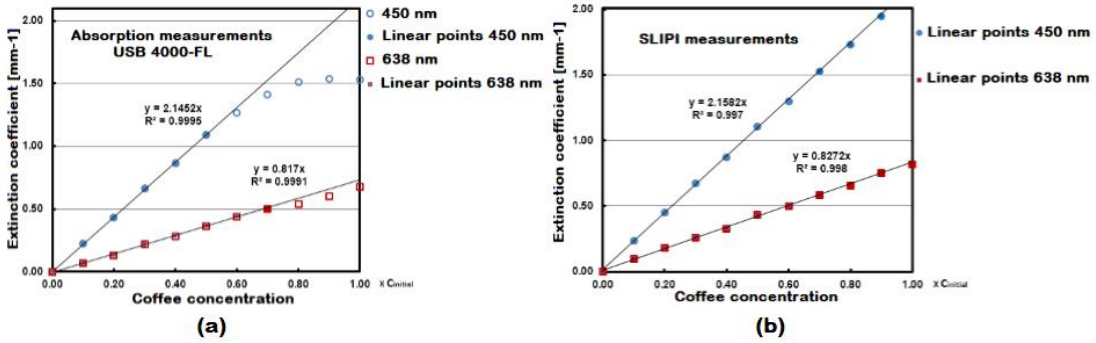

Graph 1. Extinction coefficient results as a function of concentration for coffee solutions. The absorption measurements (a) show loose linearity, while the SLIPI results (b) show good linearity.

3.2 Milk Results

The spectra acquired with the USB 4000-FL spectrometer are shown in Figure 7 (a). The resulting images of the SLIPI-1p measurements are given in Figure 7 (b). The dilution cases of solutions 6 to 10 are shown here at 450 nm. In graphs 2 (a) and 2 (b), the evolution of the extinction coefficient as a function of the concentration has been plotted for the spectroscopic and SLIPI measurements respectively.

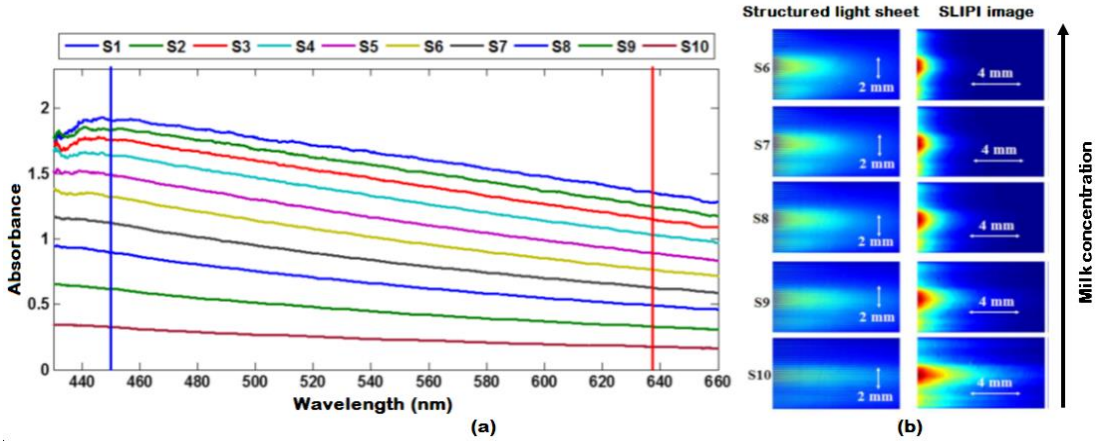

Figure 7. Absorbance spectra of the milk solutions measured using absorption spectrophotometry in (a). The increase of the absorbance with concentration is clearly seen. In (b), images of the structured light sheet crossing the cuvette at increased milk concentration. The corresponding SLIPI images are given on the right-hand side.

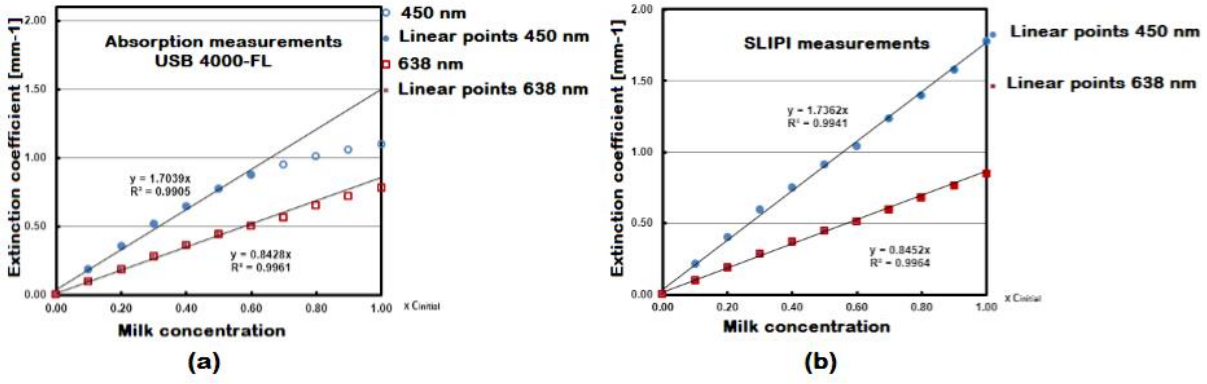

Graph 2. Extinction coefficient results as a function of concentration for milk solutions. The absorption measurements (a) show loose linearity, while the SLIPI results (b) show good linearity.

3.3 Separation of Absorption and Scattering Coefficients of Milk and Coffee Solutions

The results of the Spectroscopic and SLIPI measurements are shown in graphs 1(a) and 1(b) respectively for the coffee solutions. The SLIPI results show very good linearity between extinction coefficient and concentration at 450 nm and 638 nm wavelengths. Also, for spectroscopic measurements, the linearity is preserved when the extinction coefficient value is lower than 1.27 mm^{-1} for 450 nm illumination wavelength. It is the same case when the extinction coefficient is lower than 0.5 mm^{-1} at 638 nm illumination wavelength. In this case, the measured extinction coefficient values are very similar between the single phase SLIPI and spectroscopic measurements.

From the solution S_5 (coffee solution), the deviation between the measured value and its linear trend is remarkable at 450 nm (see graph 1(a)). This can be explained by the appearance of multiple light scattering effects. The approximation of the single scattering regime is no longer valid.

From the linear extrapolation, the absorption coefficient of this solution is determined. We have:

$$\mu_{a5} = 2.1452 * C_5 \tag{11}$$

Thus, $$\mu_{a5} = 1.2871\ mm^{-1}$$

The scattering coefficient of the solution S_5 at 450 nm is:

$$\mu_{e5\_SLIPI} = \mu_{a5} + \mu_{s5} \tag{12}$$

$$\mu_{s5} = \mu_{e5\_SLIPI} + \mu_{a5}$$

$$\mu_{s5} = 1.3004 - 1.2871$$

$$\mu_{s5} = 0.0133\ mm^{-1}$$

It is therefore this solution that will be used to make a correlation measurement and determine the scattering coefficients of the other diffuse solutions S_1, S_2, S_3 and S_4 at 450 nm.

The SLIPI measurements indicate a linearity between the values of the extinction coefficients and the concentration. Based on graph 1(b), we have:

$$\mu_{e5} = 2.1582 * C_5 = 2.1582 * 0.6 * C_1 \tag{13}$$

$$\mu_{e4} = 2.1582 * C_4 = 2.1582 * 0.7 * C_1 \tag{14}$$

Dividing relation (14) by the relation (13), its leads to:

$$\mu_{e4} = 7/6\mu_{e5}$$

By decomposing the extinction coefficients we obtain the following equation:

$$\mu_{s4} + \mu_{a4} = 7/6\mu_{a5} + 7/6\mu_{s5}\ 7/6\mu_{s5}$$

According to Narasimhan et al (Narasimhan et al., 2006), the extinction, absorption and scattering coefficients are respectively proportional to the concentration of the medium. This leads to:

$$\mu_{a4} = 7/6\mu_{a5} \tag{15}$$

$$\mu_{s4} = 7/6\mu_{s5} \tag{16}$$

Finaly, we obtain

$$\mu_{e4} = 0.0155\ mm^{-1}$$

Table 3 summarises the values of the absorption and scattering coefficients of coffee solutions illuminated at 450 nm.

Table 3. Absorption and scattering coefficients of coffee solutions at 450 nm

	Absorption coefficient μ_a(mm^{-1})	Scattering coefficient μ_s(mm^{-1})	SLIPI extinction coefficient (mm^{-1})	$\mu_a + \mu_s$ (mm^{-1})	Error (%)
S_1	2.1452	0.0221	2.1795	2.1673	0.5597
S_2	1.9306	0.0199	1.9462	1.9505	0.2106
S_3	1.7162	0.0177	1.7401	1.7339	0.3563
S_4	1.5016	0.0155	1.5264	1.5171	0.6092
S_5	1.2871	0.0133	1.3004	1.3004	0
S_6	1.0925	≈ 0	1.1067	1.0925	1.2831
S_7	0.8674	≈ 0	0.8745	0.8674	0.8118
S_8	0.6642	≈ 0	0.6727	0.6642	1.2635
S_9	0.4330	≈ 0	0.4496	0.4330	3.6921
S_{10}	0.2233	≈ 0	0.2383	0.2233	6.2946

The absorption and scattering coefficients of coffee solutions at 638 nm are determined from the solution S_3 for which the shift is high (see graph 1(b)). It will be used for the determination of the scattering coefficients of solutions S_1 and S_2 by using the same process described above.

The SLIPI results obtained from the milk solutions (see graph 2(b)), indicate a linearity between the extinction coefficient and the concentration for 450 nm and 638 nm wavelengths. This is not the case for the spectroscopic measurements, where linearity is lost for an extinction coefficient value greater than 0.76 mm^{-1} at 450 nm and 0.5 mm^{-1} at 638 nm.

Proceeding as in the previous case, the absorption and scattering coefficients of the milk solutions are determined. The separation of the coefficients will be made from the solution S_4, for which the deviation between the measured value and its linear trend is large.

Table 4 summarises the values of the absorption and scattering coefficients of milk solutions illuminated at 638 nm.

Table 4. Absorption and scattering coefficients of milk solutions at 638 nm

	Absorption coefficient μ_a(mm^{-1})	Scattering coefficient μ_s(mm^{-1})	SLIPI extinction coefficient (mm^{-1})	$\mu_a + \mu_s$ (mm^{-1})	Error (%)
S_1	0.00062	0.8428	0. 8499	0.8434	0.7647
S_2	0.00055	0.7585	0. 7658	0.7591	0.8749
S_3	0.00049	0.6742	0. 6801	0.6747	0.7940
S_4	0.00043	0.59537	0. 5958	0.5958	0
S_5	≈ 0	0.5056	0. 5103	0.5056	0.9210
S_6	≈ 0	0.4392	0. 4511	0.4392	2.6379
S_7	≈ 0	0.3590	0. 3657	0.3590	1.8321
S_8	≈ 0	0.2809	0. 2818	0.2809	0.3193
S_9	≈ 0	0.1882	0. 1886	0.1882	0.2120
S_{10}	≈ 0	0.0990	0. 1002	0.0990	1.1976

4. Discussion

The main objective of this work was to determine separately the absorption and scattering coefficients of optically dense liquid media, seat of the multiple light scattering phenomenon. Coffee and milk solutions were used for their absorbing and scattering properties respectively. The determination of these different coefficients

was done using two illumination wavelengths: 450 nm and 638 nm respectively for coffee and milk solutions. Specially, 638 nm is often used (632.8 nm or 633 nm) for the study of milk scattering solutions because of its high penetration (Moes, van-Gemert, Star, Marijnissen, & Prahl, 1989; Abegaze, 2017; Etana, 2014). Two techniques have been used:

The first technique, based on single phase SLIPI approach, allows the extinction coefficients measurement of each solution whatever its turbidity.

The second technique of spectroscopy, allows to have access by approximation, to the absorption or scattering coefficient of each solution in the linearity area depending to the nature of the medium.

The results of the absorption and scattering coefficients are presented in Tables 3 and 4 respectively for the coffee and milk solutions. The analysis of these results gives rise to some observations.

For high turbidity solutions, the linearity is lost for spectroscopy measurements (graphs 1(a) and 2(a)). This effect shows that the scattering phenomenon now plays a significant role in the extinction of light. This would explain the possibility of measuring the scattering coefficients at 450 nm of the coffee solutions from S_1 to S_5, but with low values (see Table 3).

When comparing the values of the absorption and scattering coefficients obtained at 638 nm for milk solutions with some previous studies (Gwamuri, Gholap, Shartir, & Bauh-Bassuah, 2014; Mohamed, 2000), it is observed that the absorption coefficients are similar but slightly higher than those reported in the literature for the last four milk solutions (see Table 4). This difference can be explained by several factors: (1) the quality of the milk used, (2) the milk manufacturing process (about 9.6% fat in our case), and (3) the sampling. These factors would undoubtedly lead to differences in particle concentration and size distribution.

Furthermore, this difference could also be attributed to the fact that these four solutions exhibit strong scattering. The use of the single-phase SLIPI approach has made it possible to perform reliable measurements of their optical properties by effectively suppressing the contribution of multiple light scattering, unlike conventional techniques.

Additionally, when comparing the results obtained with those of the recent studies by Adepo et al. (2024), it is observed that the values of the absorption and scattering coefficients for coffee at 450 nm and milk at 638 nm are practically similar. This correspondence highlights the consistency of the measurements obtained with our experimental approach and confirms the robustness of our method.

In previous studies, the commonly used methods were based on transmission measurements combined with fluence rate measurements. These techniques, without any approximation, allow the separation of the coefficients. In our case, if no approximation had been made, the absorption coefficients of each solution in the linear part would have been of the same order as those reported in the literature. It should also be noted that, in the case of milk solutions, the measured absorption coefficients are mainly due to water absorption (Gwamuri, Gholap, Shartir, & Bauh-Bassuah, 2014 ; Mohamed, 2000).

The sum of the absorption and scattering coefficients for each solution is approximately equal to the value of the extinction coefficient obtained from single phase SLIPI technique (see Tables 3 and 4). This confirms that the spectrometer-SLIPI combination method is a reliable technique for separating absorption and scattering coefficients.

For each coffee and milk solution, the albedo a, which is defined as the ratio between the scattering coefficient and the extinction coefficient, was calculated. Its expression is given by the following relationship:

$$a = \mu_s/(\mu_a + \mu_s) \tag{17}$$

For coffee solutions, the albedo is between 0 and 0.01. For milk solutions, the albedo is between 0.993 and 1. This confirms the fact that milk solutions are purely scattering, whereas coffee solutions are purely absorbing.

5. Conclusion

In this study, we successfully measured the absorption and scattering coefficients of strongly absorbing and scattering media, separating these properties using a novel combination of the Structured Laser Illumination Planar Imaging (SLIPI) technique and conventional optical spectroscopy. By employing a continuous wave He-Ne laser beam source at 450 nm and 638 nm, we accurately determined the extinction coefficient and subsequently deduced the absorption and scattering coefficients. The SLIPI technique effectively mitigated the effects of multiple scattering, while the spectroscopic analysis provided complementary insights, enabling precise characterization of optically dense liquid media.

This work highlights the potential of combining single-phase SLIPI and spectroscopy for diagnosing complex media, particularly in applications where distinguishing absorption from scattering is critical. However, the study has limitations that should be addressed in future research. For instance, the methodology was applied to liquid media with relatively uniform turbidity, and its applicability to more complex, heterogeneous systems remains to be explored. Additionally, the use of only two laser wavelengths constrains the spectral analysis; expanding the range of wavelengths could provide a more comprehensive understanding of the media's optical properties.

Looking forward, this approach opens several avenues for future research. The integration of single-phase SLIPI with advanced spectroscopic techniques, such as hyperspectral imaging or time-resolved spectroscopy, could further enhance the characterization of turbid media. Moreover, applying this methodology to industrial and biomedical fields, such as food quality control or tissue diagnostics, could provide valuable insights and improve measurement accuracy. By addressing the aforementioned limitations, future studies could expand the scope of this technique and contribute to the advancement of optical characterization methods in various domains.

Acknowledgments

The authors wish to thank the International Science Program (ISP) of Uppsala University for equipment and financial support as well as the Lund Laser Center (LLC).

Authors' contributions

Dr. **Guy-Oscar Regnima** was responsible for conceptualization, data curation, formal analysis, investigation, methodology, resources, and validation, as well as writing the original draft and its review and editing. Mr. **Serge Martial Adepo** contributed to formal analysis, investigation, methodology, resources, validation, and participated in writing, reviewing, and editing the manuscript. Mr. **Evariste Kouamé Amany** was involved in data curation, resources, methodology, and writing the original draft. Dr. **Thomas Koffi** and Dr. **Michel Abaka Kouacou** contributed to data curation, formal analysis, and writing the original draft. Prof. **Thouakesseh Jérémie Zoueu** was responsible for methodology, project administration, supervision, and funding acquisition, as well as writing, reviewing, and editing the manuscript. All authors read and approved the final version of the manuscript.

Funding

This work was supported by the Swedish International Development Cooperation Agency (SIDA) through the International Science Programme (ISP) at Uppsala University.

Competing interests

The authors declare that they have no known competing financial interests or personal relationships that could have influenced the work presented in this article.

Informed consent

Obtained.

Ethics approval

The Publication Ethics Committee of the Canadian Center of Science and Education.

The journal and publisher adhere to the Core Practices established by the Committee on Publication Ethics (COPE).

Provenance and peer review

Not commissioned; externally double-blind peer reviewed.

Data availability statement

The data that support the findings of this study are available on request from the corresponding author. The data are not publicly available due to privacy or ethical restrictions.

Data sharing statement

No additional data are available.

Open access

This is an open-access article distributed under the terms and conditions of the Creative Commons Attribution

license (http://creativecommons.org/licenses/by/4.0/).

Copyrights

Copyright for this article is retained by the author(s), with first publication rights granted to the journal.

References

Abegaze, W. A. (2017). Determination of fat and protein content of milk using He-Ne laser light scattering. *Doctoral dissertation*, Departement of Physics, Addis Ababa University, Addis Ababa, Ethiopia.

Adepo, S. M., Bosson, J. M., Regnima, G. O., Dion, S. B., Koffi, T., Abaka, M. K., & Zoueu, T. J. (2024). Structured Laser Illumination Planar Imaging (SLIPI): Separating the Absorption and Scattering Coefficients Using Kubelka-Munk Relationship. *Open Journal of Applied Sciences, 14*, 3441-3459. https://doi.org/10.4236/ojapps.2024.1412225

Anderson, E. R., Cuccia, D. J., & Durkin, A. J. (2007). Detection of bruises on Golden Delicious apples using spatial-frequency-domain imaging, *SPIE Conference Procedings* 6430, 643010. https://doi.org/10.1117/12.717608

Bagui, O. K., Kaduki, K. A., Berrocal, E., & Zoueu, J. T. (2016). Structured laser illumination planar imaging based classification of ground coffee using multivariate chemometric analysis. *Applied Physics Research*, 8(3), 32-44. https://doi.org/10.5539/apr.v8n3p32

Cuccia, D., Bevilacqua, F., Durkin, A., & Tromberg, B. (2005). Modulated imaging: quantitative analysis and tomography of turbid media in the spatial-frequency domain, *Optics Letters*, *30*, 1354-1356. https://doi.org/10.1364/ol.30.001354

Cuccia, D., Bevilacqua, F., Durkin, A., Ayers, F., & Tromberg, B. (2009). Quantitation and mapping of tissue optical properties using modulated imaging, *Journal of Biomedical Optics*, *14*(2), 024012. https://doi.org/10.1117/1.3088140

Davidson, S. R. H., Weersink, R. A., Haider, M. A., Gertner, M. R., Bogaards, A., Giewercer, D., … Wilson, B. C. (2009). Treatment planning and dose analysis for interstitial photodynamic therapy of prostate cancer, *Physics in Medicine and Biology*, *54*(8), 2293-2313. https://doi.org/10.1088/0031-9155/54/8/003

Delpy D. T., & Cope, M. (1997). Quantification in tissue near-infrared spectroscopy, *Philosophical Transactions of the Royal Society of London. Series B*, *352*(1354), 649-659. https://doi.org/10.1098/rstb.1997.0046

Dognitz, N., & Wagnieres, G. (1998). Determination of tissue optical properties by steady-state spatial frequency-domain reflectometry. *Lasers in Medical Science*, *13*, 55-65. https://doi.org/10.1007/BF00592960

Durduran, T., Choe, R., Baker, W. B., & Yodh, A. G. (2010). Diffuse optics for tissue monitoring and tomography. *Reports on Progress in Physics*, *73*(7). https://doi.org/10.1088/0034-4885/73/7/076701

Etana, S. K. (2014). Measurement of Turbid Body Optical Properties Using Attenuation of Laser Light Intensity Techniques. *Science, Technology and Arts Research*, *3*(1), 53-56. https://doi.org/10.4314/star.v3i1.10

Gwamuri, J., Gholap, A. V., Shartir, T. S. M., & Bauh-Bassuah, P. K. (2014). Investigating light propagation in turbid media by evaluating optical properties of phantom tissues. Retrieved from https://www.researchgate.net/publication/268402864

Hu, D., Fu, X., He, X., & Ying, Y. (2016). Noncontact and Wide-Field Characterization of the Absorption and Scattering Properties of Apple Fruit Using Spatial-Frequency Domain Imaging, *Scientific Reports*, *6*(37920). https://doi.org/10.1038/srep37920

Ishimaru, A. (1978). *Wave Propagation and Scattering in Random Media, Chapters 7 and 9*. Academic Press ed. New York.

Johansson, A., Axelsson, J., Andersson-Engels, S., & Swartling, J. (2007). Realtime light dosimetry software tools for interstitial photodynamic therapy of the human prostate, *Medical Physics*, *4*(11), 4309-4321. https://doi.org/10.1118/1.2790585

Kienle, A., Lilge, L., Patterson, M. S., Hibst, R., Steiner, R., & Wilson, B. C. (1996). Spatially resolved absolute diffuse reflectance measurements for noninvasive determination of the optical scattering and absorption

coefficients of biological tissue. *Applied Optics*, *35*, 2304-2314. https://doi.org/10.1364/AO.35.002304

Koffi, T., Bosson, J., Kouacou, A., Regnima, G.-O., Dion, S., Edo é M., Bagui, O., & Zoueu, J. T. (2019). Dense solutions' extinction coefficients measurements strategy, based on laser sheet double structuring. *Measurement*, *150*, 107089-107099. https://doi.org/10.1016/j.measurement.2019.107089

Koffi, T., Regnima, G.-O., Bosson, J., Bagui, O., Edo é, M., & Zoueu, J. T. (2017). Structured Imagery Processing Strategies for Spectroscopic Measurement in Dense Solutions. *Journal of Applied Sciences*, *7*, 262-281. https://doi.org/10.4236/ojapps.2017.76022

Kristensson, E., Araneo, L., Berrocal, E., Manin, J., Richter, M., Aldén, M., & Linne, M. (2011). Analysis of multiple scattering suppression using structured laser illumination planar imaging in scattering and fluorescing media. *Optics Express*, 19, 13647. https://doi.org/10.1364/OE.19.013647

Lu, Y., Li, R., & Lu, R. (2016). Structured-illumination reflectance imaging (SIRI) for enhanced detection of fresh bruises in apples. *Postharvest Biology and Technology*, *117*, 89-93. https://doi.org/10.1016/j.biosystemseng.2019.01.014

Meade, M. L. (1982). Advances in lock-in amplifiers. *Journal of Physics E: Scientific Instruments*, *15*, 395-403. https://doi.org/10.1088/0022-3735/15/4/001

Ménard, O., Ahmad, S., Rousseau, F., Briard-Bion, V., Gaucheron, F., & Lopez, C. (2010). Buffalo vs. cow milk fat globules: size distribution, zeta-potential, compositions in total fatty acids and in polar lipids from the milk fat globule membrane. *Food Chem*istry, *120*(2), 544-551. https://doi.org/.1016/j.foodchem.2009.10.053

Michels, R., Foschum, F., & Kienle, A. (2008). Optical properties of fat emulsions. *Optics Express*, *16*(8), 5907-5925. https://doi.org/10.1364/OE.16.005907

Mishra, Y. N., Abou, F.N., Polster, S., Kristensson, E., & Berrocal, E. (2016). Thermometry in aqueous solutions and sprays using two-color LIF and structured illumination. *Optics Express*, *24*, 4949-4963. https://doi.org/10.1364/OE.24.004949

Moes, C. J. M., van-Gemert, M. J. C., Star, W. M., Marijnissen, J. P. A., & Prahl, S. A. (1989). Measurements and calculations of the energy fluence rate in a scattering and absorbing phantom at 633 nm. *Applied Optics*, *28*(12), 2292-2296. https://doi.org/10.1364/AO.28.002292

Mohamed, T. S. (2000). Investigating Laser light Iinteraction by studying Photon Propagation and Optical Imaging through a Medium with Embedded Inhomogeneities. *Doctoral dissertation*, Cape Coast University, Cape Coast, Ghana.

Moore, C. M., Mosse, C. A., Allen, C., Payne, H., Emberton, M., & Bown, S. G. (2011). Light penetration in the human prostate: a whole prostate clinical study at 763 nm. *Journal of Biomedical Optics*, *16*(1). https://doi.org/.1117/1.3528638

Narasimhan, S. G., Gupta, M., Donner, C., Ramamoorthi, R., Nayar, S. K., & Jensen, H. W. (2006). Acquiring Scattering Properties of Participating Media by Dilution. *ACM Transactions Graphics (Proceedings SIGGRAPH)*, *25*(3), 1003-1012. https://doi.org/10.1145/1141911.1141986

Nichols, M. G., Hull, E. L., & Foster, T. H. (1997). Design and testing of a white-light, steady state diffuse reflectance spectrometer for determination of optical properties of highly scattering systems. *Applied Optics*, *36*, 93-104. https://doi.org/10.1364/AO.36.000093

Pantelides, M. L., Whitehurst, C., Moore, J. V., King, T. A., & Blacklock, N. J. (1990). Photodynamic therapy for localised prostatic cancer: light penetration in the human prostate gland. *Journal of Urology*, *43*(2), 398-401. https://doi.org/10.1016/s0022-5347(17)39973-1

Patterson, M. S., Chance, B., & Wilson, B. C. (1989). Time resolved reflectance and transmittance for the non-invasive measurement of tissue optical properties. *Applied Optics*, *28*, 2331-2336. https://doi.org/10.1364/AO.28.002331

Patterson, M. S., Moulton, J. D., Wilson, B. C., Berndt, K. W., & Lackowicz, J. R. (1991). Frequency-domain reflectance for determination of the scattering and absorption properties of tissue. *Applied Optics*, *30*, 4474-4476. https://doi.org/10.1364/AO.30.004474

Patterson, M. S., Wilson, B. C., & Wyman, D. R. (1991). The propagation of optical radiation in tissue I. Models of radiation transport and their application. *Lasers in Medical Science*, *6*(2), 155-168. https://doi.org/10.1007/BF02032543

Patterson, M. S., Wilson, B. C., & Wyman, D. R. (1991). The propagation of optical radiation in tissue II. Optical properties of tissues and resulting fluence distributions. *Lasers in Medical Science*, *6*, 379-390. https://doi.org/10.1007/BF02042460

Prahl, S. A., & Vitkin, I. A. (1992). Determination of optical properties of turbid media using pulsed photothermal radiometry. *Physics in Medicine and Biology*, *37*, 1203-1217. https://doi.org/10.1088/0031-9155/37/6/00

Regnima, G.-O., Koffi, T., Bagui, O., Kouacou, A., Kristensson, E., Zoueu, J., & Berrocal, E. (2017). Quantitative measurements of turbid liquids via structured laser illumination planar imaging where absorption spectrophotometry fails. *Applied Optics*, *56*(13), 3929-3938. https://doi.org/10.1364/AO.56.003929

Regnima, G-O., Beti é A., Koffi T., Bagui O.K., Fofana, I., Kouacou, A., & Zoueu, J. T. (2017). Monitoring power transformers oils deterioration using structured laser illumination planar imaging. *Measurement*, *113*. https://doi.org/10.1016/j.measurement.2017.08.019

Star, W. M. (1997). Light dosimetry in vivo. *Physics in Medicine and Biology*, *42*(5), 763-787. https://doi.org/10.1088/0031-9155/42/5/003

Staveren, H. J. V., Moes, C. J. M., Marie, J. V., Prahl, S. A., & Gemert, M. J. C. V. (1991). Light scattering in Intralipid-10% in the wavelength range of 400–1100 nm. *Applied Optics*, *30*(31), 4507-4514. https://doi.org/10.1364/AO.30.004507

Talbot, H. F. (1836). Facts relating to optical science. No. IV. *Philosophical Magazine*, *9*(56), 401-407. https://doi.org/10.1080/14786443608649032

Wilson, B. C., Patterson, M. S., & Burns, D. M. (1986). Effect of photosensitizer concentration in tissue on the penetration depth of photoactivating light. *Lasers in Medical Science*, *1*(4), 235-244. https://doi.org/10.1007/BF02032418

Yoon, G., Ghosh, R. D. N., & Straight, R. C. (1993). Coherent backscattering in biological media: measurement and estimation of optical properties. *Applied Optics*, *32*, 580-585. https://doi.org/10.1364/AO.32.000580

Zaccanti, G., Bianco, S. D., & Martelli, F. (2003). Measurements of optical properties of high-density media. *Applied Optics*, *42*(19), 4023-4030. https://doi.org/10.1364/AO.42.004023